J|A|C|S
ARTICLES
Published on Web 06/06/2007

Dissecting the Proline Effect: Dissociations of Proline Radicals Formed by Electron Transfer to Protonated Pro-Gly and Gly-Pro Dipeptides in the Gas Phase

Shigeo Hayakawa,[†] Mami Hashimoto,[†] Hiroshi Matsubara,[†] and František Tureček*[,‡]

Contribution from the Department of Chemistry, Graduate School of Science, Osaka Prefecture University, 1-1, Gakuencho, Nakaku, Sakai, Osaka 599-8531, Japan, and Department of Chemistry, Bagley Hall, Box 351700, University of Washington, Seattle, Washington 98195-1700

Received February 21, 2007; E-mail: turecek@chem.washington.edu

Abstract: We report a combined experimental and computational study of the proline effect in model dipeptides Pro-Gly and Gly-Pro. Gas-phase protonated peptide ions were discharged by glancing collisions with potassium or cesium atoms at 3 keV collision energies, and the peptide radical intermediates and their dissociation products were analyzed following collisional ionization to anions. The charge reversal ($^+CR^-$) mass spectra of (Pro-Gly + H)$^+$ (**1a**$^+$) and (Gly-Pro + H)$^+$ (**2a**$^+$) showed dramatic differences and thus provided a sensitive probe of ion structure. Whereas **1a**$^+$ completely dissociated upon charge inversion, **2a**$^+$ gave a nondissociated anion as the most abundant product. Ab initio and density functional theory calculations provided structures and vertical recombination energies (RE_{vert}) for **1a**$^+$ and **2a**$^+$. The recombination energies, RE_{vert} = 3.07 and 3.36 eV for **1a**$^+$ and **2a**$^+$, respectively, were lower than the alkali metal ionization energies and indicated that the collisional electron transfer to the peptide ions was endoergic. Radical **1a**$^\bullet$ was found to exist in a very shallow local energy minimum, with transition state energies for loss and migration of H indicating very facile dissociation. In contrast, radical **2a**$^\bullet$ was calculated to spontaneously isomerize upon electron capture to a stable dihydroxycarbinyl isomer (**2e**$^\bullet$) that can undergo consecutive and competitive isomerizations by proline ring opening and intramolecular hydrogen atom transfers to yield stable radical isomers. Radical **2e**$^\bullet$ and its stable isomers were calculated to have substantial electron affinities and thus can form the stable anions that were observed in the $^+CR^-$ mass spectra. The calculated TS energies and RRKM kinetic analysis indicated that peptide N−C$_\alpha$ bond dissociations compete with pyrrolidine ring openings triggered by radical sites at both the N-terminal and C-terminal sides of the proline residue. Open-ring intermediates were found in which loss of an H atom was energetically preferred over backbone dissociations. This provided an explanation for the proline effect causing low incidence of electron capture dissociations of N−C$_\alpha$ bonds adjacent to proline residues in tryptic peptides and also for some peculiar behavior of proline-containing protein cation-radicals.

Introduction

Ion−electron and ion−ion recombinations in multiply protonated peptide and protein ions produce cation radicals that undergo various dissociations. Of these, perhaps the most important and interesting are bond cleavages between amide nitrogen atoms and α carbon atoms of the C-terminal amino acid residues, the N−C$_\alpha$ cleavage.[1] When an N−C$_\alpha$ cleavage results in a fragmentation of the peptide cation-radical, it produces sequence-specific fragment ions that are important for the identification or structure elucidation of the peptide of interest.[2] A notable exception is due to proline residues in peptide and protein ions that have the special property of their N−C$_\alpha$ bonds being incorporated in pyrrolidine rings and thus their cleavages cannot result in immediate fragmentation. This proline effect has been recognized early on[2] and has been considered a minor but essential shortcoming of electron-based methods of peptide ion fragmentations such as electron capture (ECD)[3] and electron-transfer dissociations (ETD).[4]

From a mechanistic point of view, one can postulate various dissociations occurring in proline residues following electron capture or transfer. For example, Cooper et al. reported fragment ions upon ECD of doubly protonated GGPSarGGGK-NH_2 peptide ions that were attributed to fragmentations in the proline ring.[5] However, such dissociations do not seem to occur frequently or predictably,[6] as for example model peptides

[†] Osaka Prefecture University.
[‡] University of Washington.

(1) Zubarev, R. A.; Kelleher, N. L.; McLafferty, F. W. *J. Am. Chem. Soc.* **1998**, *120*, 3265−3266.
(2) Zubarev, R. A.; Horn, D. M.; Fridriksson, E. K.; Kelleher, N. L.; Kruger, N. A.; Lewis, M. A.; Carpenter, B. K.; McLafferty, F. W. *Anal. Chem.* **2000**, *72*, 563−573.
(3) (a) Zubarev, R. A. *Mass Spectrom. Rev.* **2003**, *22*, 57−77. (b) Cooper, H. J.; Hakansson, K.; Marshall, A. G. *Mass Spectrom. Rev.* **2005**, *24*, 201−222.
(4) Coon, J. J.; Ueberheide, B.; Syka, J. E. P.; Dryhurst, D. D.; Ausio, J.; Shabanowitz, J.; Hunt, D. F. *Proc. Natl. Acad. Sci. U.S.A.* **2005**, *102*, 9463−9468.
(5) (a) Cooper, H. J.; Hudgins, R. R.; Håkansson, K.; Marshall, A. G. *Int. J. Mass Spectrom.* **2003**, *228*, 723−728. (b) Cooper, H. J.; Hudgins, R. R.; Hakansson, K.; Marshall, A. G. *J. Am. Soc. Mass Spectrom.* **2002**, *13*, 241−249.

10.1021/ja0712571 CCC: $37.00

Scheme 1

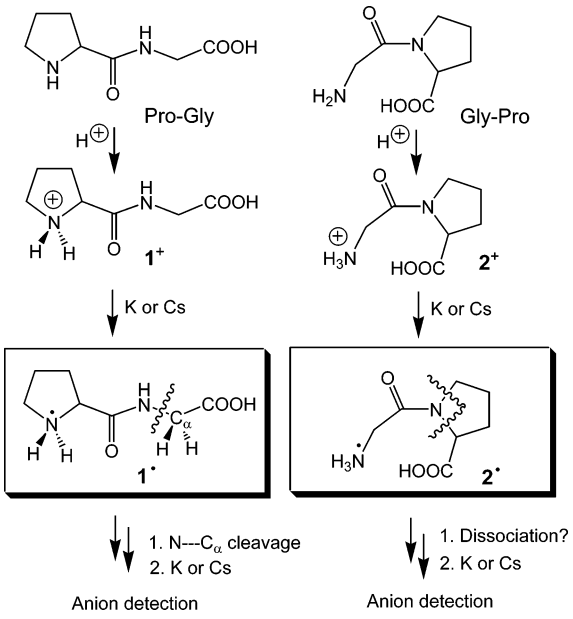

LLLLPLLLLK, GGGPGGGK, and LLLPLLLR did not show proline fragments, whereas GGGPGGGR did.[5] Hence, the proline ring cleavage may depend on the presence in the peptide ion of other specific amino acid residues, peptide conformation, or other factors affecting the dissociation mechanism(s). Hidden proline rearrangements may play a role in the unusual behavior of multiply charge protein ions upon electron capture.[7] For example, Breuker at al. reported that long-lived $(M + 12H)^{11+\bullet}$ ions from ubiquitin, a 74-residue protein containing three proline residues (P19, P37, and P38),[8] underwent exclusive loss of hydrogen atoms following activation.[7] Although those authors argued that the effect was due to an unusual reaction dynamics,[7] one may note that loss of H is the preferred dissociation of aminoketyl radicals,[9] that may be formed as stable intermediates at proline residues in long-lived $(M + 12H)^{11+\bullet}$ ubiquitin ions.

In general, mass spectrometric methods that are based on the detection of fragment ions of the same polarity as the precursor ions are not very suitable for the elucidation of the nature of the proline effect, because few structure-carrying fragments are usually observed and their structures are mostly unknown. We report a fundamentally different approach to studying the proline effect that is based on charge-inversion experiments in combination with ab initio and density functional theory calculations including large basis sets and electron correlation effects. Proline-containing peptides Pro-Gly and Gly-Pro are used as simple model systems to demonstrate this approach. The peptides are protonated in the gas phase to form singly charged ions ($\mathbf{1}^+$ and $\mathbf{2}^+$, respectively, Scheme 1) that are selected by mass, accelerated to a high velocity (5.75×10^4 m s^{-1}), and discharged by femtosecond electron transfer from an alkali metal atom (K or Cs). The intermediate radicals undergo dissociations on a time scale which is limited by the experimental observation window of 6.95×10^{-7} s. In the case of $\mathbf{1}^\bullet$, the dissociations may involve N−C_α bond cleavage to give rise to observable fragments. In $\mathbf{2}^\bullet$ the N−C_α bond is part of the pyrrolidine ring and its dissociation would result in radical isomerization but not a change of mass. The neutral intermediates and their dissociation and isomerization products are collisionally ionized by electron transfer from another alkali metal atom, the resulting anions are separated by kinetic energy and detected. Analysis of the anion mass spectra is used to characterize the products of Pro-Gly and Gly-Pro radical dissociations and isomerizations.

The essential feature of this approach is based on the fact that anion stability is very sensitive to the molecular structure and electronic properties of the neutral counterpart,[10] and thus, only anions that have substantial electron binding energies are detected. The stabilities of a number of potential structures for radical intermediates and products formed from $\mathbf{1}^\bullet$ and $\mathbf{2}^\bullet$ and the corresponding anions can be inferred from quantum chemistry calculations of adequate quality to identify the species that can give rise to the experimental mass spectra. Thus, the method has the potential of detecting even hidden rearrangements, insofar as they substantially change the product electronic properties without changing its mass. In addition to shedding new light on the proline effect, the present work can be placed in a broader context of computational studies of hydrogen rearrangements in peptide radicals and their role in biology that have been of considerable recent interest.[11,12]

Experimental Section

Methods and Materials. The MS/MS instrument used in this work comprised a double-focusing mass spectrometer (Hitachi M80B) as MS−I to mass separate precursor ions, a 4 cm long collision cell, and a toroidal electrostatic analyzer having a 216 mm central radius as MS−II to mass analyze secondary ions.[13] Dipeptides were introduced into the ionization chamber by a direct inlet probe and protonated by chemical ionization (CI) with $C_4H_9^+$/isobutane as the reactant. The formed ions were accelerated to 2970 eV, mass selected by MS−I, and focused on a collision cell filled with alkali metal vapor. The alkali metal target was supplied from a reservoir through a ball valve. Collisionally activated dissociation (CAD) spectra were measured by mass-analyzing the positive ions exiting the collision cell by scanning the MS−II. Charge reversal ($^+CR^-$) mass spectra were measured by mass-analyzing the negative ions exiting the collision cell only by altering the polarity of MS−II and the detector. The detector was 10 kV post-acceleration secondary electron multiplier, which could detect both positive and negative ions upon application of a suitable polarity. In the charge inversion process, neutralization, dissociation, and negative ion formation took place in the collision cell. Whereas mass analysis of the precursor ions provided a high resolution by double focusing mass spectrometer of MS−I, mass analysis of the fragment ions did not provide a high resolution solely by means of analysis in the electric sector of MS−II. *N*-Prolylglycine (Pro-Gly) and *N*-glycylproline (Gly-

(6) Leymarie, N.; Berg, E. A.; McComb, M. E.; O'Connor, P. B.; Grogan, J.; Oppenheim, F. G.; Costello, C. E. *Anal. Chem.* **2002**, *74*, 4124−4132.
(7) Breuker, K.; Oh, H.-B.; Lin, C.; Carpenter, B. K.; McLafferty, F. W. *Proc. Natl. Acad. Sci. U.S.A.* **2004**, *101*, 14011−14016.
(8) Schlesinger, D. H.; Goldstein, G.; Niall, H. D. *Biochemistry* **1975**, *14*, 2214−2218.
(9) (a) Syrstad, E. A.; Stephens, D. D.; Tureček, F. *J. Phys. Chem. A* **2003**, *107*, 115−126. (b) Tam, F.; Syrstad, E. A.; Chen, X.; Tureček, F. *Eur. J. Mass Spectrom.* **2004**, *10*, 869−879. (c) Al-Khalili et al. *J. Chem. Phys.* **2004**, *121*, 5700−5708.
(10) Harrison, A. G. *Chemical Ionization Mass Spectrometry*, 2nd ed.; CRC Press: Boca Raton, FL, 1992.
(11) (a) Wood, G. P. F.; Easton, C. J.; Rauk, A.; Davies, M. J.; Radom, L. *J. Phys. Chem. A* **2006**, *110*, 10316−10323. (b) Rauk, A.; Yu, D.; Armstrong, D. A. *J. Am. Chem. Soc.* **1998**, *120*, 8848−8855. (c) Reid, D. L.; Armstrong, D. A.; Rauk, A.; Nese, C.; Nien Schuchmann, M.; Westhoff, U.; von Sonntag, C. *Phys. Chem. Chem. Phys.* **2003**, *5*, 3278−3288. (d) Rauk, A.; Armstrong, D. A. *J. Am. Chem. Soc.* **2000**, *122*, 4185−4192. (e) Rauk, A.; Armstrong, D. A.; Fairlie, D. P. *J. Am. Chem. Soc.* **2000**, *122*, 9761−9767. (f) Rauk, A.; Yu, D.; Taylor, J.; Shustov, G. V.; Block, D. A.; Armstrong, D. A. *Biochemistry* **1999**, *38*, 9089−9096.
(12) Moran, D.; Jacob, R.; Wood, G. P. F.; Coote, M. L.; Davies, M. J.; O'Hair, R. A. J.; Easton, C. J.; Radom, L. *Helv. Chim. Acta* **2006**, *89*, 2254−2272.
(13) Hayakawa, S. *Int. J. Mass Spectrom.* **2001**, *212*, 229−247.

Pro) were purchased from Kokusankagaku, Japan and used as received. Isobutane (Takachiho, Japan) gas was also used as received.

Calculations. Standard ab initio calculations were performed using the *Gaussian 03* suite of programs.[14] Optimized geometries were obtained by density functional theory calculations using Becke's hybrid functional (B3LYP)[15] and the 6-31++G(d,p) basis set. The optimized structures are shown in the pertinent schemes and figures. Complete optimized structures of local minima are available as Supporting Information or can be obtained from the corresponding author upon request. Spin unrestricted calculations were performed for all open-shell systems. Stationary points were characterized by harmonic frequency calculations with B3LYP/6-31++G(d,p) as local minima (all real frequencies) and first-order saddle points (one imaginary frequency). The calculated frequencies were scaled[16] with 0.963 and used to obtain zero-point energy corrections, enthalpies, and entropies. The rigid-rotor-harmonic-oscillator (RRHO) model was used in thermochemical calculations except for low-frequency modes where the vibrational enthalpy terms that exceeded 0.5 RT were replaced by free internal rotation terms equal to 0.5 RT.

Improved energies were obtained by single-point calculations that were carried out at several levels of theory, including split-valence triple-ζ basis sets of increasing size furnished with polarization and diffuse functions, e.g., 6-311++G(2d,p), and 6-311++G(3df,2p). For the molecular system of Gly-Pro radical size, the larger basis set comprised 598 symmetry-adapted basis functions. The spin unrestricted formalism was used for calculations of open-shell systems. Contamination by higher spin states was modest, as judged from the expectation values of the spin operator $\langle S^2 \rangle$ that were ≤ 0.76 for UB3LYP and ≤ 0.78 for UMP2 calculations. The UMP2 energies were corrected by spin annihilation[17] that reduced the $\langle S^2 \rangle$ to close to the theoretical value for a pure doublet state (0.75). Spin annihilation lowered the total MP2 energies by 6 millihartree (15.7 kJ mol^{-1}, root-mean-square deviation) for local energy minima and transition states. The B3LYP and MP2 energies calculated with the large basis set were combined according to the B3−MP2 scheme, as described previously for peptide radical systems.[18] The total energies are compiled in Table S1 (Supporting Information).

The performance of the B3−PMP2 scheme was tested on a set of pyrrolidine cations and radicals by comparing several relative, dissociation, and transition-state energies with those obtained by coupled-cluster calculations[19] with singles, doubles, and disconnected triples, CCSD(T).[20] The single-point energies were extrapolated from a linear expansion of polarization *d* and *f* functions in the basis set (eq 1).

$$E[\text{CCSD(T)/6-311++G(3df,2p)}] \approx E[\text{CCSD(T)/6-311++G(d,p)}] + E[\text{PMP2/6-311++G(3df,2p)}] - E[\text{PMP2/6-311++G(d,p)}] \quad (1)$$

Table S2 (Supporting Information) shows that the B3−MP2 relative and transition state energies were within 2.0 kJ mol^{-1} (root-mean-square deviation) of the CCSD(T) data. Thus, the B3−PMP2 scheme was deemed satisfactory for calculations of the larger Pro-Gly and Gly-Pro peptide radicals for which large-scale CCSD(T) single-point calculations were beyond our computational resources. Atomic spin and charge densities were calculated using the Natural Population Analysis (NPA) method.[21]

Unimolecular rate constants were calculated according to the Rice-Ramsperger-Kassel-Marcus (RRKM) theory[22] using Hase's program[23] that was recompiled and run under Windows XP.[24] RRKM rate constants were obtained by direct count of quantum states at internal energies that were increased in 2 kJ mol^{-1} steps from the transition state up to 300 kJ mol^{-1} above it. Rotations were treated adiabatically, and the calculated $k(E,J,K)$ microscopic rate constants were Boltzmann-averaged over the thermal distribution of rotational states at 500 K, corresponding to the ion source temperature, to provide canonical rate constants $k(E)$. Formal kinetic analysis of consecutive and competitive dissociations was carried out using the method of Laplace transforms.[25]

Results and Discussion

Ion Formation and Structures. Gas-phase protonation of dipeptides Gly-Pro and Pro-Gly produced singly charged ions $\mathbf{1}^+$ and $\mathbf{2}^+$. The energetics of proton transfer from the CI reagent and the ion structures are critical for the formation of the radicals of interest and therefore are addressed first.

Gas-phase structures for the starting Gly-Pro and Pro-Gly dipeptides were obtained by B3LYP/6-31++G(d,p) optimizations and confirmed to be local minima by harmonic vibrational analysis. The presence of the rigid proline residue greatly simplifies the conformational space for both dipeptides to include structures **GP-I**, **GP-II**, **GP-III**, **PG-I**, **PG-II**, and **PG-III** that have favorable bond dipole−dipole interactions or intramolecular hydrogen bonding (Figure 1). The *trans*-amide isomer **GP-III** was found to be most stable of the GP conformers, followed by the *cis*-amides **GP-II** and **GP-I** (Table 1). We note that the hydrogen bonding between the Pro-COOH and Gly amide carbonyl group in **GP-III** decreased both the enthalpy and entropy of the peptide and thus diminished the difference in free energy relative to **GP-I**. At the ion source temperature (500 K), we calculate $\Delta G^\circ_{g,500}$(**GP-I** → **GP-III**) = −1.9 kJ mol^{-1} which gives 61% **GP-III** and 39% **GP-I** at gas-phase equilibrium.[26−28] In contrast, **PG-III** was found to be the thermochemically and thermodynamically most stable isomer among the Pro-Gly conformers and was expected to dominate (>96%) in a gas-phase equilibrium at the ion source temperature (500 K).

(14) Frisch, M. J.; et al. *Gaussian 03*, revision B.05; Gaussian, Inc.; Pittsburgh PA, 2003.
(15) (a) Becke, A. D. *J. Chem. Phys.* **1993**, *98*, 1372−1377. (b) Becke, A. D. *J. Chem. Phys.* **1993**, *98*, 5648−5652. (c) Stephens, P. J.; Devlin, F. J.; Chabalowski, C. F.; Frisch, M. J. *J. Phys. Chem.* **1994**, *98*, 11623−11627.
(16) Rauhut, G.; Pulay, P. *J. Phys. Chem.* **1995**, *99*, 3093−3100.
(17) (a) Schlegel, H. B. *J. Chem. Phys.* **1986**, *84*, 4530−4534. (b) Mayer, I. *Adv. Quantum Chem.* **1980**, *12*, 189−262.
(18) (a) Tureček, F. *J. Phys. Chem. A* **1998**, *102*, 4703−4713. (b) Tureček, F.; Polášek, M.; Frank, A. J.; Sadílek. M. *J. Am. Chem. Soc.* **2000**, *122*, 2361−2370. (c) Polášek, M.; Tureček, F. *J. Am. Chem. Soc.* **2000**, *122*, 9511−9524. (d) Tureček, F.; Yao, C. *J. Phys. Chem. A* **2003**, *107*, 9221−9231. (e) Rablen, P. R. *J. Am. Chem. Soc.* **2000**, *122*, 357−368. (f) Rablen, P. R. *J. Org. Chem.* **2000**, *65*, 7930−7937. (g) Rablen, P. R.; Bentrup, K. H. *J. Am. Chem. Soc.* **2003**, *125*, 2142−2147. (h) Hirama, M.; Tokosumi, T.; Ishida, T.; Aihara, J. *Chem. Phys.* **2004**, *305*, 307−316.
(19) Čížek, J.; Paldus, J.; Šroubková, L. *Int. J. Quantum Chem.* **1969**, *3*, 149−167.
(20) Purvis, G. D.; Bartlett, R. J. *J. Chem. Phys.* **1982**, *76*, 1910−1918.
(21) Reed, A. E.; Weinstock, R. B.; Weinhold, F. *J. Chem. Phys.* **1985**, *83*, 735−746.
(22) Gilbert, R. G.; Smith, S. C. *Theory of Unimolecular and Recombination Reactions*; Blackwell Scientific Publications: Oxford, 1990; pp 52−132.
(23) Zhu, L.; Hase, W. L. *Quantum Chemistry Program Exchange;* Indiana University: Bloomington, 1994; Program No. QCPE 644.
(24) Frank, A. J.; Sadílek, M.; Ferrier, J. G.; Tureček, F. *J. Am. Chem. Soc.* **1997**, *119*, 12343−12353.
(25) Connors, K. A. *Chemical Kinetics*; VCH: New York, 1990; pp 82−90.
(26) Neutral Gly-Pro is likely to exist as a mixture of cis and trans-amide isomers (ref 27). From the experimental activation parameters for the cis-trans amide isomerization in peptides containing the GP motif ($\Delta H^\ddagger = 91.2$ kJ mol^{-1} and $\Delta S^\ddagger = 29.3$ J mol^{-1} K^{-1}), one obtains the isomerization rate constant as $k = 1.05 \times 10^5$ s^{-1} at 500 K. Similar activation parameters follow from computational studies referring to the gas phase (ref 28). The mean residence time for the gaseous neutral peptide molecules in the high-pressure ion source (3−4 ms) is 350−450 isomerization half-lives, implying that **GP-I** and **GP-III** can rapidly interconvert in the ion source prior to ionization.
(27) Shi, T.; Spain, S. M.; Rabenstein, D. L. *J. Am. Chem. Soc.* **2004**, *126*, 790−796.
(28) (a) Kang, Y. K.; Jhon, J. S.; Park, H. S. *J. Phys. Chem. B* **2006**, *110*, 17645−17655. (b) Kang, Y. K. *J. Phys. Chem. B* **2006**, *110*, 21338−21348. (c) Jhon, J. S.; Kang, Y. K. *J. Phys. Chem. B* **2007**, *111*, 3496−3507. (d) Kang, Y. K.; Choi, H. Y. *Biophys. Chem.* **2004**, *111*, 135−142. For recent reviews, see: (e) Wedemeyer, W. J.; Welker, E.; Scheraga, H. A. *Biochemistry* **2002**, *41*, 14637−14644. (f) Pielak, G. J. *Protein Sci.* **2006**, *15*, 393−394.

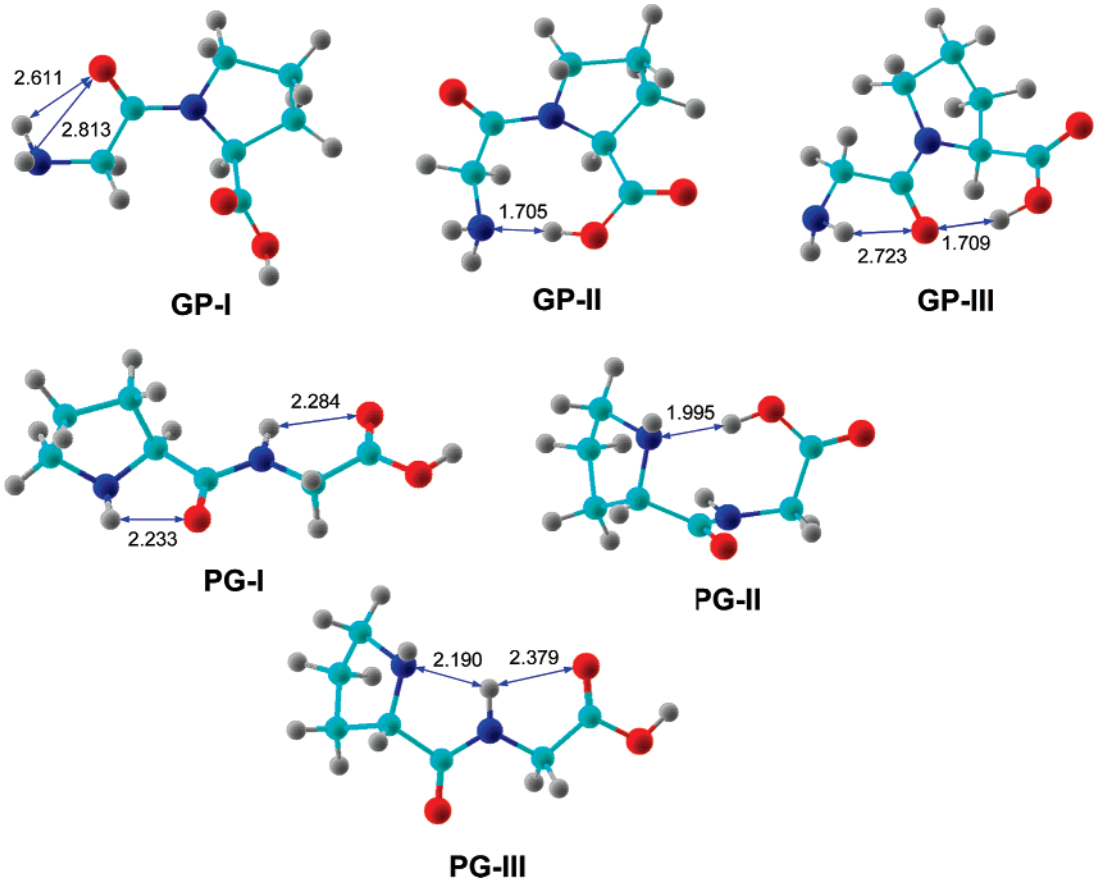

Figure 1. B3LYP/6-31++G(d,p) optimized structures of peptides Pro-Gly and Gly-Pro. Double arrows show intramolecular hydrogen bonds in angstroms.

Table 1. Peptide Neutral and Ion Relative Energies

species/reaction	relative energy[a,b] B3LYP 6-31++G(d,p)	B3–MP2 6-311++G(2d,p)	B3–MP2 6-311++G(3df,2p)
PG-I → **PG-II**	23 (30)[c]	20 (27)[c]	20 (27)[c]
PG-I → **PG-III**	−11 (−9.5)[c]	−10 (−9)[c]	−9 (−8)[c]
GP-I → **GP-II**	−3.4 (5.9)[c]	−1.5 (7.7)[c]	−0.8 (8.5)[c] (16.3)[d]
GP-I → **GP-III**	−14 (−8.1)[c]	−13 (−6.4)[c]	−13 (−6.7)[c] (−1.9)[d]
$\mathbf{1a}^+ \rightarrow$ **PG-III** + H^+	972	967	968
$\mathbf{1a}^+ \rightarrow \mathbf{1b}^+$	31	31	30
$\mathbf{2a}^+ \rightarrow$ **GP-II** + H^+	953	950	952
$\mathbf{2a}^+ \rightarrow$ **GP-III** + H^+	942	939	940
$\mathbf{2a}^+ \rightarrow \mathbf{2b}^+$	34	34	35 (33)[c] (32)[d]
$\mathbf{2a}^+ \rightarrow \mathbf{2b_{OH}}^+$	37	41	42 (40)[c] (36)[d]
$\mathbf{2a}^+ \rightarrow \mathbf{2c}^+$	60	55	59
$\mathbf{2a}^+ \rightarrow \mathbf{2d}^+$	81	78	79

[a] In units of kJ mol^{-1}. [b] Including B3LYP/6-31++G(d,p) zero-point energies and 298 K enthalpies and referring to 298 K. [c] 298 K free energies. [d] 500 K free energies.

Protonation in Pro-Gly can be expected to occur at the basic proline N-terminus to give pyrrolidinium cations.[29] Out of these, ion $\mathbf{1a}^+$ had the pyrrolidinium group internally solvated to the amide group at a 1.762 Å H···O distance (Figure 2). Ion $\mathbf{1a}^+$ was found to be more stable than its conformer $\mathbf{1b}^+$ in which the H-bonding was to the carboxyl group (Figure 2, Table 1). The proton affinity of **PG-III** was calculated to be PA = 968 kJ mol^{-1} when forming the most stable ion $\mathbf{1a}^+$. Protonation in Gly-Pro was considered to occur either at the glycine N-terminus or in the proline pyrrolidine ring (Figure 2). Out of the ion

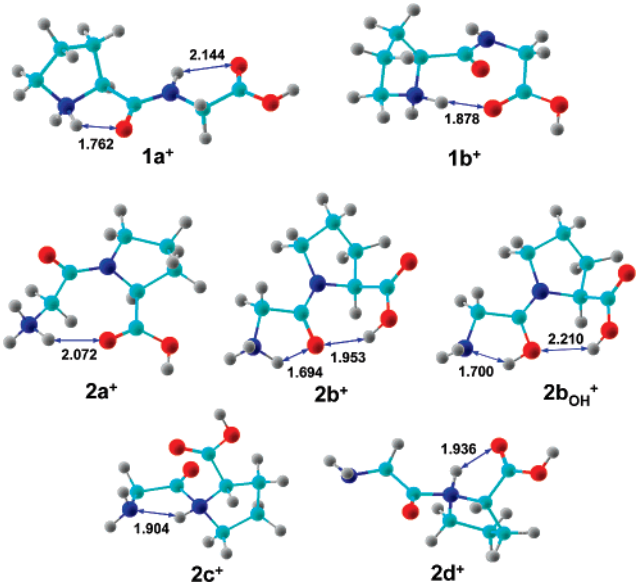

Figure 2. B3LYP/6-31++G(d,p) optimized structures of peptide cations from Pro-Gly and Gly-Pro. Double arrows show intramolecular hydrogen bonds in angstroms.

structures, the Gly protonated and internally solvated *cis*-amide ion $\mathbf{2a}^+$ was found to be substantially more stable than the *trans*-amide ion $\mathbf{2b}^+$, its tautomer $\mathbf{2b_{OH}}^+$, and the Pro-protonated ions $\mathbf{2c}^+$ and $\mathbf{2d}^+$ (Table 1). The proton affinities of **GP-I** and **GP-III** when forming $\mathbf{2a}^+$ and $\mathbf{2b}^+$ were calculated to be PA = 952 and 905 kJ mol^{-1}, respectively. Due to the different basicities of **GP-I** and **GP-III**, the formation of $\mathbf{2a}^+$ can be

(29) (a) Harrison, A. G. *Mass Spectrom. Rev.* **1997**, *16*, 201−217. (b) Frøsig, L.; Tureček, F. *J. Am. Soc. Mass Spectrom.* **1998**, *9*, 242−254.

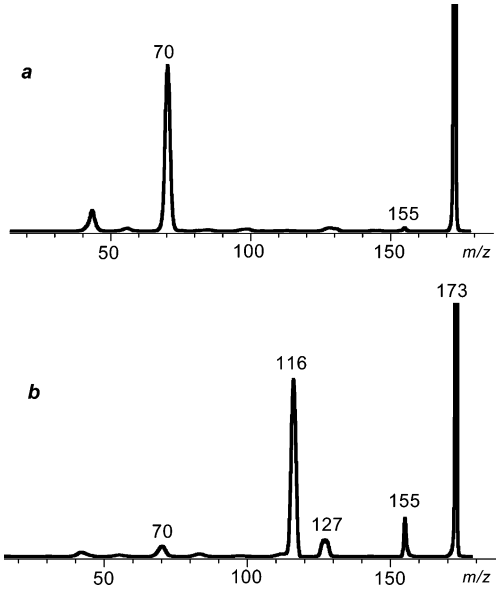

Figure 3. Collisionally activated dissociation spectra of (a) **1a**$^+$ and (b) **2a**$^+$ obtained with cesium as collision target. The peaks of precursor ions at *m*/*z* 173 are off scale.

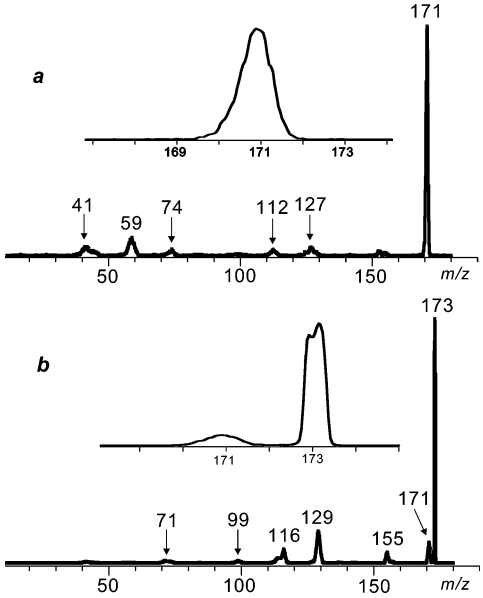

Figure 4. Charge-reversal mass spectra of (a) **1a**$^+$ and (b) **2a**$^+$ obtained with cesium as collision target. (Insets) Kinetic energy peak profiles in the $^+CR^-$ mass spectra.

viewed as proceeding by two convergent pathways, one being direct CI-protonation of **GP-I**, and the other CI-protonation of **GP-III** followed by exothermic proton transfer from **2b**$^+$ to **GP-I**.

In summary, the protonation sites in Pro-Gly and Gly-Pro are well defined by the thermodynamic properties of the most stable ion conformers. It is worth noting that **1a**$^+$ is 30 kJ mol^{-1} more stable than **2a**$^+$ when based on the calculated $\Delta G^\circ_{g,298}$.

The mean internal energies of the cations produced by isobutane chemical ionization can be estimated as follows. Proton transfer from $C_4H_9^+$ (PA(2-methylpropene) = 802 kJ mol^{-1})[30] to **PG-III** and **GP-III** is exothermic by 166 and 138 kJ mol^{-1}, respectively. The reaction exothermicity can be partitioned between the products, **1a**$^+$ or **2a**$^+$ and 2-methylpropene, roughly in the ratio of their 500 K heat capacities.[31] This gives an estimate of the upper bounds for the mean internal energy in **1a**$^+$ and **2a**$^+$ as 117 and 96 kJ mol^{-1}, respectively. The lower bounds are given by the ro-vibrational enthalpies of the ions when thermalized by multiple collisions with isobutane at the ion source temperature (500 K), e.g., 62 and 63 kJ mol^{-1} for **1a**$^+$ and **2a**$^+$, respectively. Note that the ions do not exchange internal energy during their flight between the ion source and the collision cell.

Ion Dissociations. Collisional activation of mass selected and isolated **1a**$^+$ and **2a**$^+$ resulted in ion dissociations that were monitored in positive-ion mass spectra (Figure 3a,b for collisions with Cs and Figure S1a,b, Supporting Information, for collisions with K). The ion dissociations of **1a**$^+$ (Pro-Gly) showed major products at *m*/*z* 70 and 43 that can be assigned to fragmentations in the N-terminal proline residue, as observed for other proline-containing peptides.[32] The predominant peak in the CAD spectra of **2a**$^+$ (Gly-Pro) (Figure 3b) was observed at *m*/*z* 116. This most likely corresponds to protonated proline (y_1 fragment ion),[32] which usually becomes predominant in dissociations of peptide ions having a proline residue in the C-terminal position.[33] The fragment ions giving rise to peaks at *m*/*z* 155 and 127 are formed by losses of H_2O and (H_2O + CO), respectively. Thus, the CAD spectra obtained with 3 keV precursor ions and K or Cs as collision targets showed standard dissociation patterns.

Charge Inversion in Pro-Gly (1a$^+$) and Gly-Pro (2a$^+$) Ions. The charge-reversal ($^+CR^-$) mass spectra of **1a**$^+$ and **2a**$^+$ were substantially different regardless of the collision target used, e.g., for Cs (Figure 4a,b) and K (Figure S2a,b, Supporting Information). The $^+CR^-$ spectrum of **1a**$^+$ showed a major peak at *m*/*z* 171 which indicated a loss of two H atoms or an H_2 molecule from **1a**$^+$ as a result of charge inversion. Another fragment anion was observed at *m*/*z* 59, which likely corresponded to $^-CH_2COOH$ or an isomer. The $^-CH_2COOH$ anion is known to be stable under collisional reionization,[34] and it can be formed by reionization of a $^\bullet CH_2COOH$ radical that represents a *z*-type fragment from an N−C_α bond dissociation in the neutral intermediate **1a**$^\bullet$. The complementary *c*-type fragment appeared as a small peak at *m*/*z* 112. Fragment anions were also observed at *m*/*z* 153 (171 − H_2O)$^-$, 127 (171 − CO_2)$^-$, 74 (possibly H_2NCH^-COOH), 44, and 41 that may have originated from consecutive anion dissociations. No survivor anion at *m*/*z* 173 was observed for **1a**$^+$. In sharp contrast, the charge-inversion spectrum of **2a**$^+$ was *dominated by the non-dissociated m/z* 173 anion. A few significant fragment anions were observed that were due to eliminations of molecules, e.g., *m*/*z* 171 (loss of H_2), *m*/*z* 155 (loss of water), *m*/*z* 129 (loss of CO_2), *m*/*z* 116 (loss of H_2NCHCO), *m*/*z* 114, 99, and 71.

(30) *NIST Standard Reference Database*, Number 69, June 2005 Release, http://webbook.nist.gov/chemistry.
(31) The 500 K gas-phase heat capacities (J mol^{-1} K^{-1}) were as follows: 2-methylpropene (129.35) (ref 30), **1a**$^+$ (306.08), and **2a**$^+$ (297.81).
(32) (a) Paizs, B.; Suhai, S. *Mass Spectrom. Rev.* **2005**, *24*, 508−548. (b) Wysocki, V. H.; Cheng, G.; Zhang, Q.; Herrmann, K. A.; Beardsley, R. L.; Hildebrand, A. E. Peptide Fragmentation Overview. In *Principles of Mass Spectrometry Applied to Biomolecules*, Laskin, J., Lifshitz, C., Eds.; Wiley-Interscience: Hoboken, New Jersey, 2006; Part II, Chapter 8, pp 279−300.
(33) Vaisar, T.; Urban, J. *J. Mass Spectrom.* **1996**, *31*, 1185−1187.
(34) Vivekananda, S.; Sadílek, M.; Chen, X.; Tureček, F. *J. Am. Soc. Mass Spectrom.* **2004**, *15*, 1053−1067.

Scheme 2

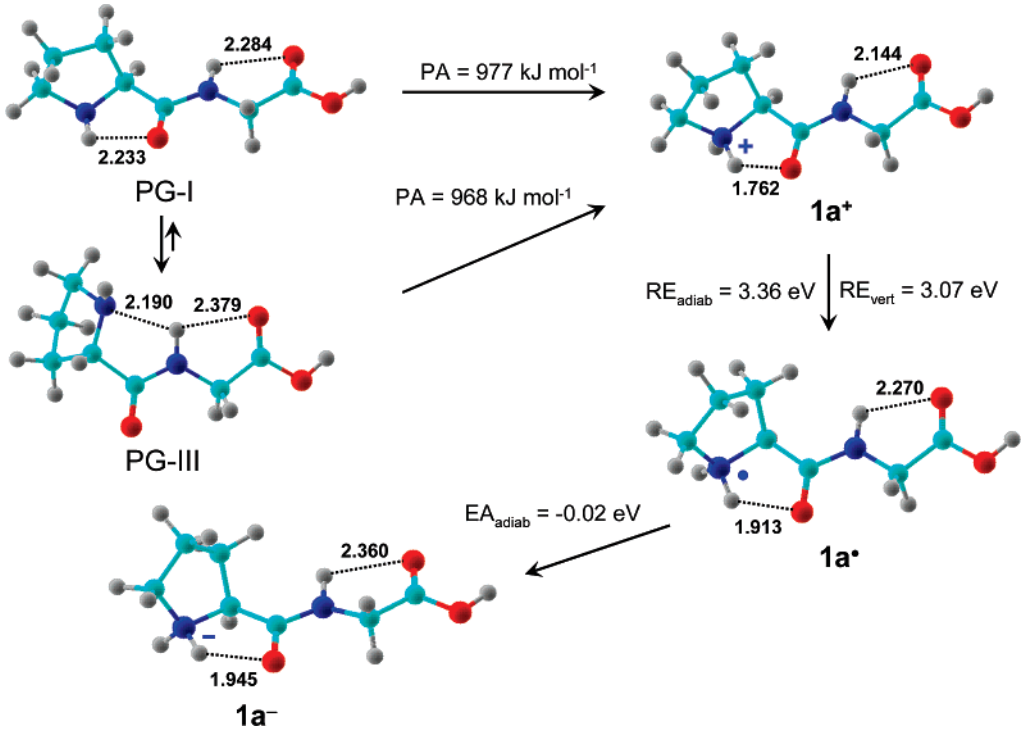

Insets in Figure 4a,b show the expanded portions of the $^{+}CR^{-}$ mass spectra of $\mathbf{1a}^{+}$ and $\mathbf{2a}^{+}$ in the *m*/*z* 167−174 region. The *m*/*z* 173 peak from $\mathbf{2a}^{+}$ shows a narrow trapezoid profile which is similar to the profile of the precursor cation beam and indicates virtually no broadening by kinetic energy release. In contrast, the *m*/*z* 171 peak from $\mathbf{1a}^{+}$ is substantially broadened and shows a Gaussian shape which indicates kinetic energy release in the fragmentation. From the *m*/*z* 171 peak width at half-maximum and after correction for the main beam width,[35−37] we obtain the kinetic energy release for loss of H_2 as $T_{0.5} = 24$ kJ mol^{-1} for charge inversion with both K and Cs. The mean kinetic energy release is $\langle T \rangle = 2.16 \times T_{0.5}$ for a pure Gaussian peak profile, giving an estimate of $\langle T \rangle \approx 52$ kJ mol^{-1}. Weak and broadened peaks at *m*/*z* 171 are also observed in the charge inversion mass spectra of $\mathbf{2a}^{+}$, indicating minor loss of H_2 or 2H from the other isomer that amount to 8% of the *m*/*z* 173 anion intensity. We note that the $^{+}CR^{-}$ mass spectra do not distinguish whether the dissociations occurred in one or more steps in the intermediate radicals **1a** and **2a**, or upon reionization to anions. For example, one step elimination of H_2 is 436 kJ mol^{-1} less endothermic than a consecutive loss of two H atoms if they occurred from the same reactant. However, a consecutive loss of two H atoms may be more favorable if the first loss occurred in the radical stage and the second in the anion stage, because each reaction can be driven by different thermochemistry.

The similarity of the $^{+}CR^{-}$ mass spectra obtained with K and Cs is significant and deserves some comment. Due to the very low ionization energies of K (4.341 eV) and Cs (3.894 eV) when compared to the typical recombination energies of organic cations (RE(ion) = 7−11 eV), electron transfer from alkali metal atoms to cations derived from standard organic molecules is usually highly exothermic[38] and results in energy deposition in the incipient neutral intermediate. In addition, cations K^{+} and Cs^{+} have high-lying excited states that are not likely to be produced upon collision. Hence, electron transfer from K or Cs is considered to be near-resonant with the appropriate vibronic state of the incipient neutral organic species.[13,39] The energy difference (ΔE) that causes excitation in the transient neutral can be expressed by eq 2, where RE(ion) is the vertical recombination energy of the cation to the ground electronic state of the corresponding neutral.

$$\Delta E = |\mathrm{IE(target)} - \mathrm{RE(ion)}| \qquad (2)$$

Because IE(Cs) < IE(K), electron transfer from Cs results in greater excitation and more extensive dissociation of the neutral intermediate, as reported for several small organic species, e.g., C_2H_2,[40] C_3H_4,[41] and dichlorobenzene.[42] Therefore, the similarity of the $^{+}CR^{-}$ spectra of $\mathbf{1a}^{+}$ and $\mathbf{2a}^{+}$ with K and Cs targets may indicate that the neutral species formed by the neutralization have very similar internal energies.

The observation of a molecular anion, as in the $^{+}CR^{-}$ mass spectrum of $\mathbf{2a}^{+}$, is highly unusual, because in charge inversion processes using alkali metal targets most neutral species formed by near-resonant neutralization dissociate spontaneously. Non-

(35) Cooks, R. G.; Beynon, J. H.; Caprioli, R. M.; Lester, G. R. *Metastable Ions*; Elsevier: Amsterdam, 1973; p 60.
(36) Holmes, J. L.; Osborne, A. D. *Org. Mass Spectrom.* **1981**, *16*, 236.
(37) Hayakawa, S.; Mori, M.; Watanabe, N.; Fujii, H.; Arakawa, K.; Morishita, N. *J. Mass Spectrom. Soc. Jpn.* **2001**, *49*, 144−149.
(38) (a) Feng, R.; Wesdemiotis, C.; Zhang, M.; Marchetti, M.; McLafferty, F. W. *J. Am. Chem. Soc.* **1989**, *111*, 1986−1991. (b) Burgers, P. C.; Kulik, W.; Versluis, C.; Terlouw, J. K. *Int. J. Mass Spectrom. Ion Processes* **1990**, *98*, 247−258.
(39) (a) Hayakawa, S.; Harada, K.; Watanabe, N.; Arakawa, K.; Morishita, N. *Int. J. Mass Spectrom.* **2000**, *202*, A1−A7. (b) Hayakawa, S. *J. Mass Spectrom.* **2004**, *39*, 111−135.
(40) Hayakawa, S.; Tomozawa, K.; Takeuchi, T.; Arakawa, K.; Morishita, N. *Phys. Chem. Chem. Phys.* **2003**, *5*, 2386−2390.
(41) Hayakawa, S.; Endoh, H.; Arakawa, K.; Morishita, N. *Int. J. Mass Spectrom. Ion Processes* **1997**, *171*, 209−214.
(42) Hayakawa, S.; Taguchi, K.; Kotani, R.; Arakawa, K.; Morishita, N. *J. Mass Spectrom. Soc. Jpn.* **2001**, *49*, 219−223.

Scheme 3

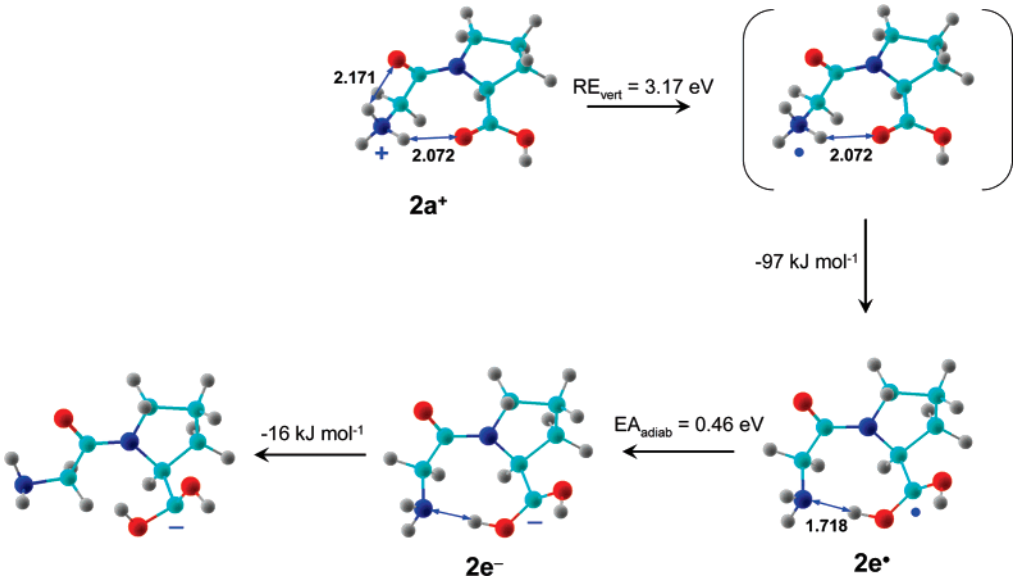

dissociated charge inverted ions were observed only for atomic,[43] C_2, and C_2H anions formed by double electron transfer in a single collision.[44] When an alkali metal is used as a target, double electron transfer in a single collision is much less probable than successive single electron transfers in two collisions, as discussed previously.[43] The previous studies indicated that most negative ions observed in $^+CR^-$ mass spectra were formed by successive single electron transfers in two collisions. However, successive electron transfer in $^+CR^-$ mass spectra often does not yield stable anions, even if the intermediate neutrals have positive electron affinities, as observed for small molecules, such as vinylidene,[45] and a few others.[46] This indicates that the dominant anion peak from **2a**$^+$ must be due to some special electronic properties of the intermediate radical.

The $^+CR^-$ mass spectra of **2a**$^+$ with K and Cs were also similar when recorded at different number densities of either target. This similarity also indicated that most charge inverted ions, including the non-dissociated ones, were formed by successive single collision processes, e.g., via one-electron transfer to the cation followed by spontaneous dissociation or isomerization of the neutrals, and endothermic electron-transfer resulting in the negative ion formation. The predominant *m*/*z* 173 peaks in the charge inversion spectra of **2a**$^+$ suggest that the structure of the anions is different from that of the precursor cation. However, because of the lack of dissociation, specific structure information is not available from the $^+CR^-$ mass spectra. Therefore, the properties of the radical intermediates and the energetics of electron transfer were addressed by quantum chemistry calculations as discussed next.

Electron Transfer to Pro-Gly (1a$^+$) and Gly-Pro (2a$^+$) Ions. We first address the structures of radicals **1a**• and **2a**• and the recombination energies of the corresponding cations **1a**$^+$ and **2a**$^+$. B3LYP/6-31++G(d,p) geometry optimizations yielded a local energy minimum for **1a**• (Scheme 2). Structure **1a**• was a hypervalent pyrrolidinium radical,[47] that showed an elongated hydrogen bonding of the in-plane pyrrolidinium proton to the amide group at 1.913 Å. The vertical and adiabatic recombination energies of **1a**$^+$ were very low, but similar, e.g., RE_{vert}(**1a**$^+$) = 3.07 eV and RE_{adiab}(**1a**$^+$) = 3.36 eV. Note that both RE values for **1a**$^+$ are lower than the ionization energies of the alkali metals, so that the electron transfer is slightly endoergic. The energy deficit is made up by conversion of a small fraction of the center-of mass kinetic energy of the two-particle system, e.g., E_{COM} = 548 and 1290 eV for collisions with K and Cs, respectively. The comparison of the ion recombination and target ionization energies indicated that the electron transfer was not near-resonant. Under such circumstances eq 2 does not apply, and the internal energy of the radical intermediate can be approximated[48] by the sum of the Franck−Condon energy acquired upon vertical electron transfer (0.3 eV, 28 kJ mol^{-1} in **1a**•) and the internal energy of the precursor cation (62−117 kJ mol^{-1} for **1a**$^+$, vide supra), giving a broad range of E_{int} = 90−145 kJ mol^{-1} for **1a**•.

Vertical electron transfer to **2a**$^+$ was associated with RE_{vert}(**2a**$^+$) = 3.17 eV, which was again lower than the ionization energies of the alkali metal targets. However, the incipient radical (**2a**•) was not a potential energy minimum, but it spontaneously isomerized by ammonium hydrogen atom migration to form radical **2e**• (Scheme 3). We note that the duration of the collisional electron transfer (~15 fs)[49,50] was comparable to the period (*T*) of the relevant ν(N−H) bond vibration in **2a**$^+$ for the migrating hydrogen atom (3190 cm^{-1}, *T* = 10 fs), and so the isomerization could occur during

(43) Hayakawa, S.; Kadomura, K.; Kimura, M.; Dutta, C. M. *Phys. Rev. A: At., Mol., Opt. Phys.* **2004**, *70*, 022708/1−022708/6.
(44) Hayakawa, S.; Terazawa, N.; Sugiura, T. *J. Phys. B: At., Mol., Opt. Phys.* **1990**, *23*, 4539−4548.
(45) Hayakawa, S.; Takahashi, M.; Arakawa, K.; Morishita, N. *J. Chem. Phys.* **1999**, *110*, 2745−2748.
(46) Hayakawa, S.; Kawamura, Y.; Takahashi, Y. *Int. J. Mass Spectrom.* **2005**, *246*, 56−64.
(47) Frøsig, L.; Tureček, F. *J. Am. Soc. Mass Spectrom.* **1998**, *9*, 242−254.
(48) (a) Wolken, J. K.; Tureček, F. *J. Am. Chem. Soc.* **1999**, *121*, 6010−6018. (b) Tureček, F. *Int. J. Mass Spectrom.* **2003**, *227*, 327−338.
(49) Estimated from the ion velocity (5.75 × 10^3 m s^{-1}) and the combined molecular dimensions of **2a**$^+$ (7.8 Å) and Slater's atomic radii for alkali metal atoms (2.2 Å for K, and 2.6 Å for Cs) (ref 50).
(50) Slater, J. C. *J. Chem. Phys.* **1964**, *41*, 3199−3204.

Table 2. Energies of Pro-Gly Radicals

species/reaction	relative energy[a,b] B3LYP 6-31++G(d,p)	B3–MP2 6-311++G(2d,p)	B3–MP2 6-311++G(3df,2p)
1a• → **PG-I** + H•	2	−21	−21
1a• → **TS1**	7	0.5	0.1
1a• → **1d•**	−55	−62	−63
1a• → **TS2**	1.5	4.2	3.3
1d• → **TS3**	45	50	52
1a• → **1e•**	−61	−68	−66
1a• → **3** + **4**	−43	−46	−45
1a• → **TS4**	19	12	11
1a• → **1f•**	−125	−128	−127
1a• → **1g•**	−93	−102	−101
1a• → **TS5**	15	21	22
1a• → **TS6**	37	46	48
1a• → **1h•** + H_2	−134	−132	−135
1a• → **TS7**	0.6	−14	−15
PG-I + H• → **TS7**	−1.5	7.7	6.6

[a] In units of kJ mol^{-1}. [b] Including B3LYP/6-31++G(d,p) zero-point corrections and referring to 0 K.

the electron transfer through a mixed vibronic state. The energy difference between **2a**$^+$ and **2e•** (4.31 eV) indicated that the overall electron transfer was near resonant with K and slightly exothermic with Cs. The further isomerizations and dissociations of the primary neutralization products **1a•** and **2e•** are treated separately by examining the relevant parts of the corresponding potential energy surfaces (PES) along the reaction pathways.

Dissociations of 1a•. Radical **1a•** was found to reside in an extremely shallow potential energy minimum. The lowest transition state for a pyrrolidinium N−H bond cleavage (**TS1**) was at $E_{TS1} = 0.1$ kJ mol^{-1} indicating facile dissociation (Table 2). The loss of H was calculated to be 21 kJ mol^{-1} exothermic to form amide **PG-I** (Scheme 4). A migration of the internally solvated pyrrolidinium H atom to the amide carbonyl through **TS2** also required a very low TS energy, e.g., $E_{TS2} = 3.3$ kJ mol^{-1}, to yield the aminoketyl radical **1d•** at −63 kJ mol^{-1} relative to **1a•**. A further N−C$_\alpha$ bond cleavage in **1d•** required 52 kJ mol^{-1} in **TS3** relative to **1d•** (Table 2). This placed **TS3** below both **TS2** and **1a•**, and hence, the subsequent N−C$_\alpha$ bond cleavage in **1d•** was expected to occur spontaneously. The N−C$_\alpha$ bond cleavage led to a dipole−dipole complex **1e•** that was practically isoenergetic with **1d•**. Separation of the incipient fragments (**3** and **4**, Scheme 4) in **1e•** required 21 kJ mol^{-1}, which placed the products' energy at −45 kJ mol^{-1} relative to **1a•**. The aminoketyl radical **1d•** can also lose the hydroxyl H atom through **TS4** that requires 11 kJ mol^{-1} relative to **1a•** (Table 2).

Cleavages of the N−C bonds in the **1a•** pyrrolidinium ring were substantially exothermic to produce open-ring intermediates **1f•** and **1g•**, respectively. The corresponding transition states, **TS5** and **TS6** (Scheme 5), were calculated to be 22 and 48 kJ mol^{-1} above **1a•**, respectively, and thus were both above **TS1**-**TS3**. It may be noted that the open-ring radicals **1f•** and **1g•** are likely to be at equilibrium with several other structures differing in the chain conformations, some of which may be more stable than the primary products of ring opening in **1a•**. The conformational space for **1f•** and **1g•** and the relevant global energy minima have not been investigated in this work. However, the ring openings in **1a•** required substantially higher TS energies (**TS5** and **TS6**) than did the loss and transfer of the pyrrolidinium H atom. This indicated that the ring openings, which would not directly lead to dissociation, were not kinetically competitive with the H atom loss resulting in the very facile dissociation of **1a•**.

The most exothermic dissociation of **1a•** was elimination of an H_2 molecule leading to radical **1h•** at −135 kJ mol^{-1} relative to **1a•**. A transition state for H_2 formation (**TS7**) was found to be at $E_{TS7} = -15$ kJ mol^{-1} relative to **1a•**. However, intrinsic

Scheme 4

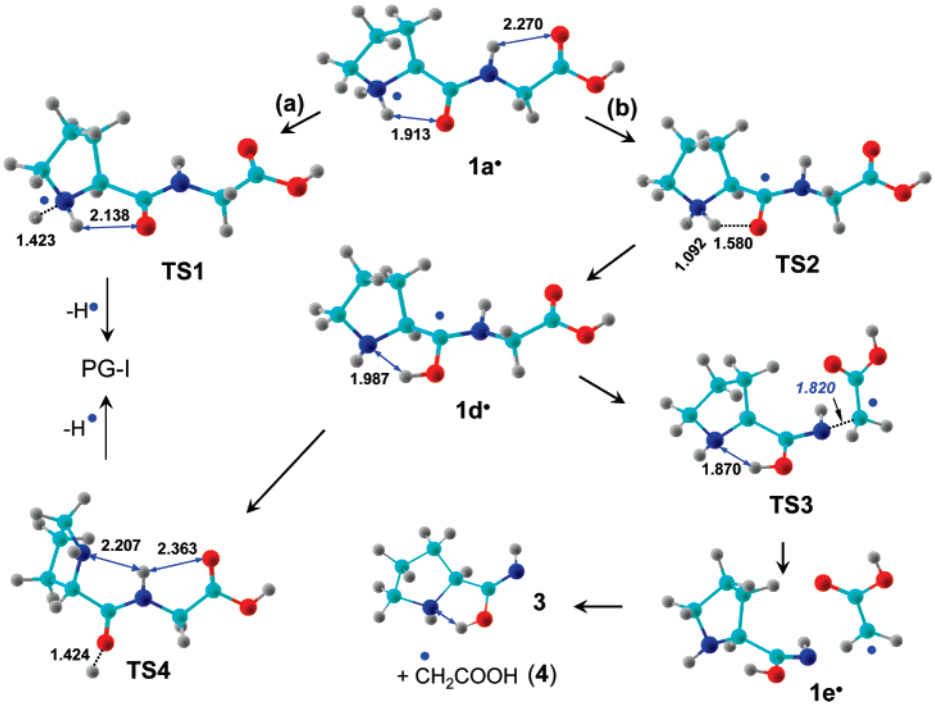

Scheme 5

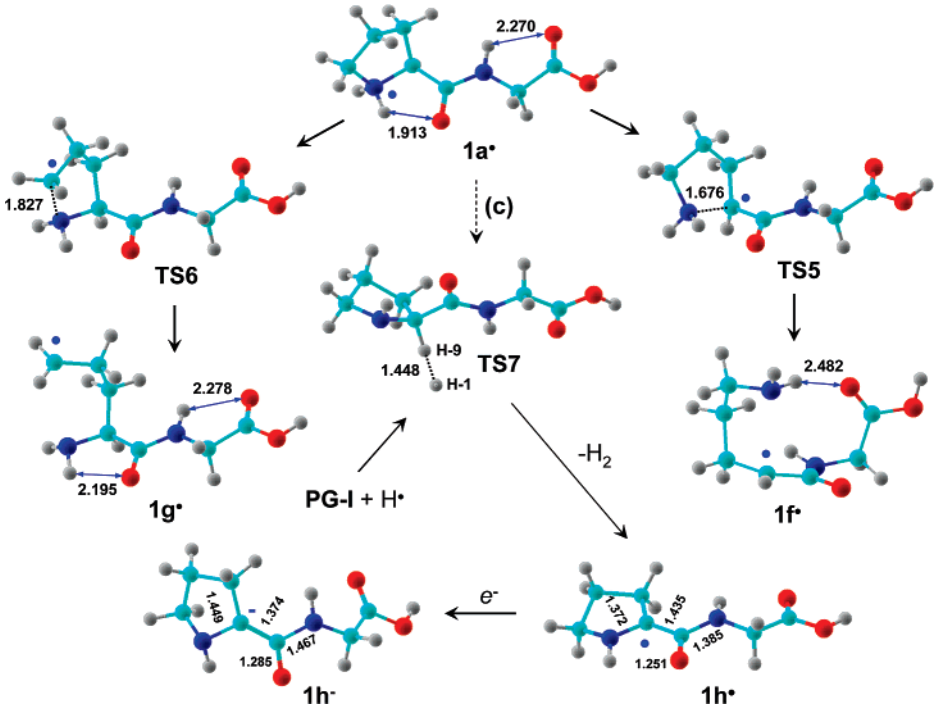

reaction coordinate analysis[51] revealed that **TS7** (Scheme 5) was not connected to **1a•**, but rather to the **PG-I** + H• reactants and thus corresponded to an H-atom abstraction by a hydrogen radical in **PG-I** rather than a unimolecular H_2 elimination in **1a•**. The **TS7** geometry (Scheme 5) showed that to connect it with **1a•**, one would have to completely interrupt the N−H bond at 3.348 Å to bring the ammonium hydrogen atom (H-1) within 1.448 Å of the proline α-hydrogen (H-9) in **TS7**. However, because the N−H-1 bond dissociation in **1a•** is *exothermic*, the departing H-1 is expected to acquire kinetic energy along the dissociation trajectory past **TS1** which points *away* from H-9. An analysis of the N···H-1 dissociation path indeed showed that the distance between H-1 and H-9 increased from 2.233 Å in **TS1** to 2.601 Å at an N···H-1 distance of 2.000 Å. Thus, the reaction pathways for the N−H-1 bond dissociation through **TS1** and the H-1···H-9−C_α abstraction through **TS7** follow divergent valleys that are separated by a bulge on the PES. The bulge was mapped by B3LYP calculations and its height was found to decrease as H-1 moved away from the pyrrolidine ring. This was also indicated by the force constant for the transversal δ(N−H) deformation vibrational mode that decreased along the same path. This leaves open a possibility for dynamic effects where, given the low barriers and sufficient internal energy in **1a•** (>90 kJ mol^{-1}, vide supra), some departing H-1 atoms may ignore the minimum energy pathways and cut the corner on the flat PES to approach **TS7** for elimination of H_2.

Dissociations of 2e•. Radical **2e•** was formed spontaneously upon electron transfer to ion **2a**$^+$ (Scheme 3). In contrast to **1a•**, **2e•** was a carbon-centered radical that resided in a substantial potential energy minimum (Table 3). The dissociations of **2e•** that were promoted by the carboxyl radical center may involve several β-fission-type bond cleavages. Loss of a hydrogen atom through **TS8** (E_{TS8} = 91 kJ mol^{-1}) formed the less stable Gly-Pro peptide conformer **GP-II** at 47 kJ mol^{-1} (Scheme 6). N−C_α cleavages in the pyrrolidine ring may also be facilitated by the radical center. The ring cleavage proceeding

Table 3. Energies of Gly-Pro Radicals

species/reaction	relative energy[a,b] B3LYP 6-31++G(d,p)	B3–MP2 6-311++G(2d,p)	B3–MP2 6-311++G(3df,2p)
2e• → **GP-II** + H•	68	45	47
2e• → **TS8**	95	91	91
2e• → **GP-III** + H•	54	33	34
2e• → **b•**	50	54	55
2e• → **2f•**	−95	−90	−89
2e• → **TS9**	40	47	50
2f• → **5** + CH_2=CHCOOH	106	120	121
2f• → **TS10**	118	122	123
2e• → **2g•**	75	75	73
2e• → **TS11**	113	115	114
2e• → **2h•**	−44	−44	−48
2e• → **TS12**	86	84	84
2e• → **2i•**	−114	−108	−108
2e• → **TS13**	19	23	25
2e• → **2j•**	−2	−4	−5
2e• → **TS14**	102	95	95
2e• → **2k•**	−11	−10	−12
2e• → **2l•**	18	17	16
2k• → **TS15**	32	34	37
2e• → **2m•**	11	8	7
2m• → **2n•**	−21	−17	−15
2m• → **TS16**	35	38	39
2n• → **6** + CH_2=CHCOOH	105	118	119
2m• → **GP-III** + H•	43	25	26
2m• → **TS17**	86	82	83
2m• → **2b•**	39	46	48
2m• → **TS18**	44	48	49
2b• → **GP-III** + H•	4	−21	−21
2b• → **TS19**	25	20	19
2b• → **7** + NH_3	−119	−127	−127
2b• → **TS20**	−3	−4	−4

[a] In units of kJ mol^{-1}. [b]Including B3LYP/6-31++G(d,p) zero-point corrections and referring to 0 K.

(51) Gonzalez, C.; Schlegel, H. B. *J. Chem. Phys.* **1989**, *90*, 2154−2161.

Table 4. Radical Electron Affinities

	electron affinity[a,b]		
species	B3LYP 6-31++G(d,p)	B3–PMP2 6-311++G(2d,p)	B3–PMP2 6-311++G(3df,2p)
1a•	0.09	−0.02	−0.02
1f•	1.63	1.62	1.66
1h•	0.62	0.69 (−0.11)[c]	0.71 (−0.04)[c]
2e•	0.43	0.43	0.46
2f•	1.96	1.95 (1.44)[c]	1.99 (1.50)[c]
2h•	1.01	1.05 (0.21)[c]	1.05 (0.28)[c]
2i•	1.01	1.07 (0.06)[c]	1.09 (0.13)[c]
2m•	0.67	0.70 (−0.15)[c]	0.72 (−0.10)[c]
2n•	1.98	2.00 (1.48)[c]	2.03 (1.54)[c]

[a] In units of electron volt. [b] Adiabatic values including B3LYP/6-31++G(d,p) zero-point corrections unless stated otherwise. [c] Vertical electron affinities with no zero-point corrections.

through **TS9** required $E_{TS9} = 50$ kJ mol^{-1} and produced the open-ring isomer **2f•**, which was 89 kJ mol^{-1} more stable than **2e•** (Scheme 6, Table 3). A noticeable feature of the ring opening was that it did not stop at an N-centered amidyl radical but continued to proceed by a migration of an ammonium hydrogen atom to form the more stable radical **2f•**. The further dissociation by $C_\beta-C_\gamma$ bond cleavage in **2f•** was 121 kJ mol^{-1} endothermic to form radical **5** and acrylic acid. The $C_\beta-C_\gamma$ bond cleavage proceeded through **TS10** which was 123 kJ mol^{-1} above **2f•** and 34 kJ mol^{-1} above the **2e** energy. Cleavage of the other pyrrolidine N−C bond in **2e•** required a higher transition state, **TS11**, $E_{TS11} = 114$ kJ mol^{-1} (Table 3), to give open-ring isomer **2g•**, which was 73 kJ mol^{-1} less stable than **2e•**.

With regard to the spatial proximity of the Gly and Pro residues in **2e•**, we also investigated H-atom migration to the C-terminal radical center. In particular, transfer of one of the Gly α-hydrogens was calculated to be 48 kJ mol^{-1} exothermic to form radical **2h•** (Scheme 7). The pertinent **TS12** was 84 kJ mol^{-1} above **2e•**, making the isomerization potentially competitive with the hydrogen atom loss and $C_\beta-C_\gamma$ bond cleavage. Another low-energy pathway was migration of a Gly α-hydrogen atom in **2f•** through **TS13** that required only a 25 kJ mol^{-1} activation energy to form another very stable isomer **2i•** (Scheme 7, Table 3).

Anion Energies. Because the product detection in the $^+CR^-$ mass spectra relied on anions, the anion stabilities were of importance. Table 4 summarizes the calculated electron affinities of the most important products and intermediates of radical **1a•** and **2e•** dissociations and isomerizations. As expected by analogy with other ammonium radicals,[52] **1a•** did not bind an additional electron in a valence state to form a stable anion. In contrast, **1f•**, **1h•**, **2e•**, **2h•**, **2i•**, and other α-radicals had substantial electron affinities and can be expected to form stable anions, e.g., **2e**$^-$ (Scheme 3), upon adiabatic electron transfer. However, the vertical electron affinity of **1h•** was close to zero, which indicated substantial Franck−Condon effects in vertical electron attachment to the radical. The optimized structures of **1h•** and **1h**$^-$ showed different bond lengths, in particular, for the proline $C_\alpha-CO$ and the amide C═O, and C−N bonds (Scheme 5) that were likely to contribute to the vibrational excitation in vertically formed anion **1h**$^-$.

(52) Boldyrev, A. I.; Simons, J. *J. Chem. Phys.* **1992**, *97*, 6621−6627.

We note that the calculated electron affinities of **1f•**, **1h•**, and **2e•**−**2n•** (Table 4) were lower than the ionization energies of the alkali metal atomic targets. Thus, the potential formations of **1f**$^-$ and **2e**$^-$−**2n**$^-$ by collisions with both K and Cs were all endoergic and would require kinetic energy conversion in an electron-transfer collision. Although we did not calculate electron affinities for the closed-shell potential products, e.g., peptides **PG-I**, **GP-II**, **GP-III**, their EA values can be safely expected to be close to zero or negative, because the amide group does not have low-lying valence states to accommodate an extra electron.

Discussion of the Radical Dissociations. We now use the above-described results of ab initio calculations to discuss the charge inversion mass spectra. To recapitulate, protonated peptide ions Pro-Gly (**1a**$^+$) and Gly-Pro (**2a**$^+$) showed dramatically different behavior upon charge inversion by collisions with alkali metal atoms. The calculations predicted that radical **1a•** was extremely weakly bound, which was consistent with the absence of a survivor anion in the $^+CR^-$ mass spectrum. Furthermore, ion **1a**$^+$ was calculated to have very low recombination energies, both vertical and adiabatic, that made the electron transfer from K and Cs mildly endoergic. This explains the insensitivity of the $^+CR^-$ mass spectra to the nature of the electron donor.

The calculations pointed to three dissociations of **1a•** that had very low transition state energies, e.g., (a) loss of a pyrrolidinium H atom, (b) H-atom migration to the amide group followed by $N-C_\alpha$ bond dissociation (Scheme 4), and (c) elimination of H_2 involving the proline pyrrolidinium and α-hydrogen atoms (Scheme 5). Dissociations (a) and (c) can both give rise to the prominent *m*/*z* 171 peak $^+CR^-$ mass spectrum of **1a**$^+$. Dissociation (a) initially forms neutral peptide **PG-I** that upon collision can undergo dissociative electron capture by loss of another H atom to form stable α-glycyl[53] or α-prolyl anions at *m*/*z* 171. Dissociation (c) would lead to radical **1h•** which is a direct precursor of the α-prolyl anion. Although we cannot distinguish paths (a) and (c) unequivocally, the properties of the relevant transition states, as described above, together with the low vertical electron affinity of **1h•** seem to disfavor path (c) to account for the *m*/*z* 171 anion.

Path (b) is indicated by the presence of the *m*/*z* 59 anion in the $^+CR^-$ mass spectrum of **1a**$^+$. This dissociation is kinetically controlled by the very low transition state energy for the pyrrolidinium H atom migration in **1a•** which is in direct competition with the loss of the other pyrrolidinium H-atom. The relative intensities of the *m*/*z* 59 and *m*/*z* 171 peaks indicate that the latter pathway (a) should be favored, in line with its lower calculated transition state energy (**TS1**). A quantitative comparison of the calculated and experimental branching ratios for paths (a) and (b) would require to determine the ionization cross sections for the anion formations and also to assess the mass-dependent ion transmission through the electrostatic sector of the tandem mass spectrometer. Such data are not available, and thus a quantitative comparison is difficult to make.

(53) (a) Tureček, F.; Carpenter, F. H.; Polce, M. J.; Wesdemiotis, C. *J. Am. Chem. Soc.* **1999**, *121*, 7955−7956. (b) Carpenter, F. H.; Tureček, F. *J. Chem. Soc. Perkin Trans. 2* **1999**, 2315−2323. (c) O'Hair, R. A. J.; Blanksby, S.; Styles, M.; Bowie, J. H. *Int. J. Mass Spectrom.* **1999**, *182/183*, 203−211.

Scheme 6

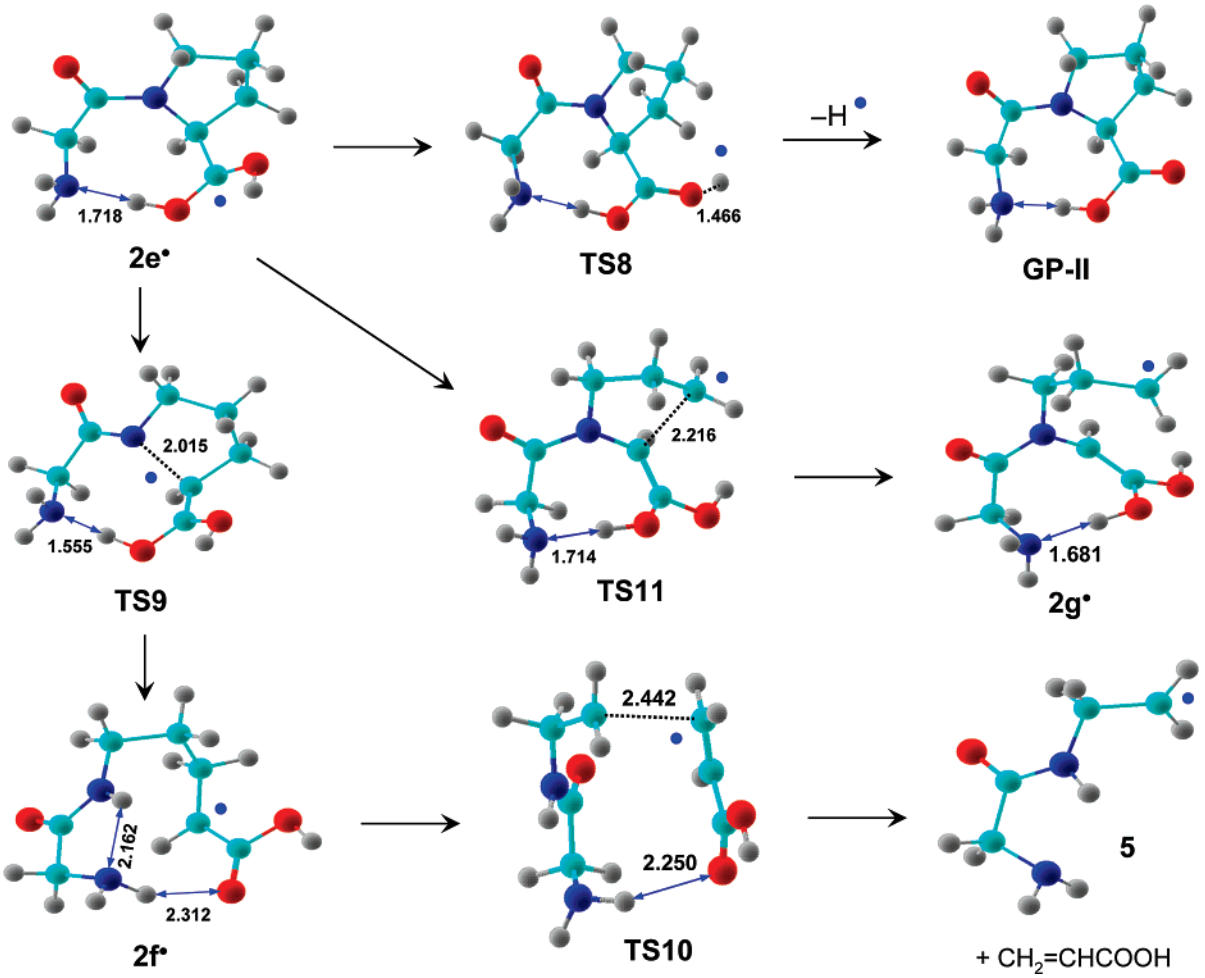

Scheme 7

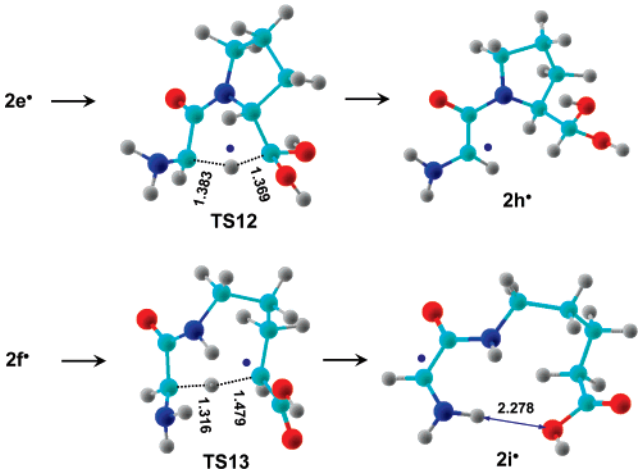

The $^{+}CR^{-}$ mass spectrum of **2a**$^{+}$ showed relatively little dissociation, in general keeping with the proline ring effect. The calculations provided an insight into the processes that led to the preservation of the intermediate radicals and the formation of stable anions. Regarding the radical intermediates, particularly interesting is the relayed hydrogen atom transfer onto the amide nitrogen atom in the course of N−C$_\alpha$ bond cleavage in the proline ring in **TS9** that leads to substantial stabilization in structure **2f•** (Scheme 6). This indicates that the proline residue may function as a *radical trap* for hydrogen atoms approaching from both the N- and C-terminus of the charge-reduced peptide cation-radical.[54] These effects are difficult to discern in standard studies using ECD and ETD and are revealed for the first time by a combination of $^{+}CR^{-}$ and theoretical investigation of the PES.

Relevance to Other Proline Containing Peptides. The above-discussed results were further expanded to include species with radical sites at both the N- and C-terminal sides of the proline residue. To this end we investigated an isomerization in **2e•** by hydrogen migration forming α-glycyl radicals (Scheme 8). A prerequisite for such an isomerization in **2e•** is rotation about the Gly−amide bond (**TS14**) to form intermediates **2j•** and **2k•**. It is worth noting that while **2j•** and **2k•** are slightly more stable than **2e•**, which makes the rotation thermodynamically favorable, it requires a substantial activation energy in **TS14** (Table 3). The $E_{\mathbf{TS14}} = 95$ kJ mol^{-1} is in line with the rotation barriers in Pro-containing peptides[27,28] and slightly higher than the rotation barriers in other tertiary amides,[12,55] possibly because of the disruption of intramolecular hydrogen bonding in the reactant **2e•** (Scheme 8). Radical **2k•** is expected

(54) (a) Belyayev, M. A.; Cournoyer, J. J.; Lin, C.; O'Connor, P. B. *J. Am. Soc. Mass Spectrom.* **2006**, *17*, 1428−1436. (b) Jones, J. W.; Sasaki, T.; Goodlett, D. R.; Turecek, F. *J. Am. Soc. Mass Spectrom.* **2007**, *18*, 432−444.

(55) (a) Le Master, C. B.; True, N. S. *J. Phys. Chem.* **1989**, *93*, 1307. (b) Wiberg, K. B.; Rablen, P. D.; Rush, D. J.; Keith, T. A. *J. Am. Chem. Soc.* **1995**, *117*, 4261−4270. (c) Kemnitz, C. R.; Loewen, M. J. *J. Am. Chem. Soc.* **2007**, *129*, 2521−2528.

Scheme 8

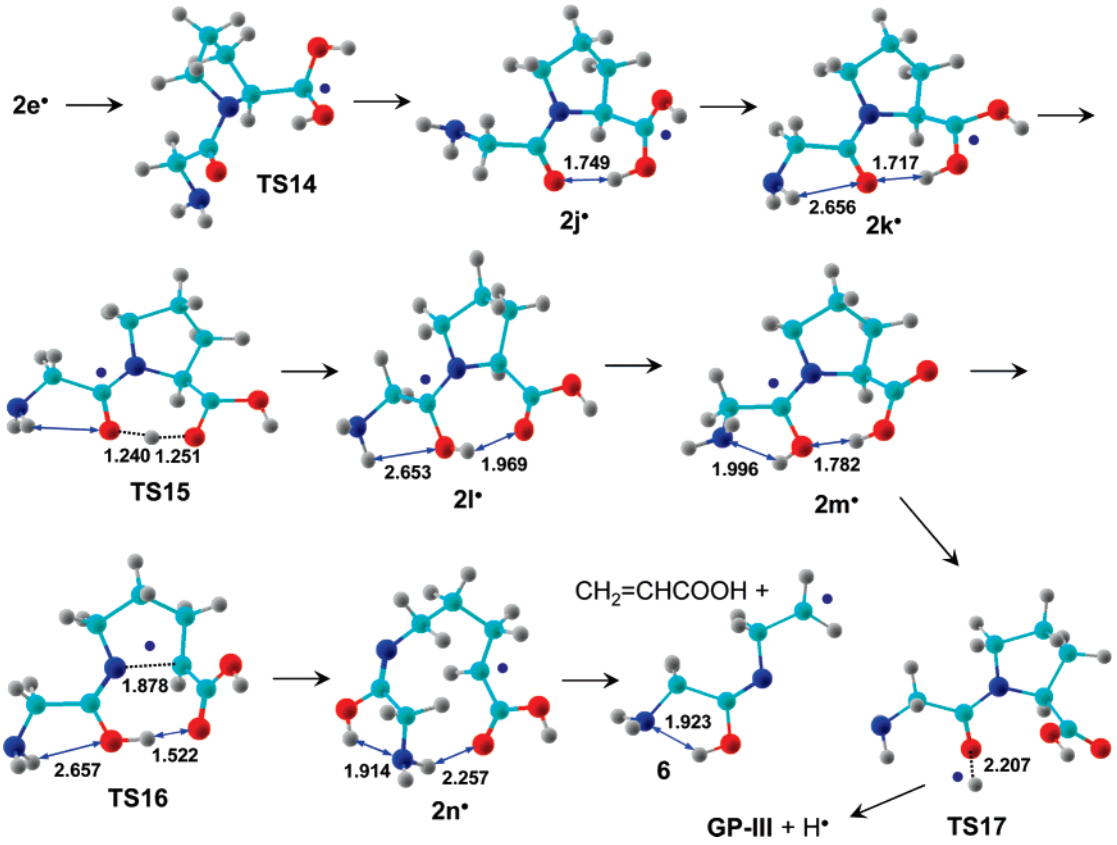

to undergo facile H-atom migration through **TS15** to form the Gly aminoketyl radical **2l•** which can gain further stabilization by isomerizing to its conformer **2m•**. The latter can undergo ring opening by N−C_α bond cleavage through **TS16** to form another stable isomer **2n•**, lose the hydroxyl H-atom through **TS17**, or isomerize to **2b•** through **TS18**. Note that the ammonium radical **2b•** is highly unstable and is prone to dissociate by practically barrierless loss of ammonia through **TS20** (Scheme S1, Supporting Information).

The calculated TS energies further indicate that the loss of hydroxyl H-atom from **2m•** (an N-terminal radical) and **2e•** (a C-terminal radical) are practically isoenergetic. A similar conclusion follows from the comparison of TS energies for the ring-opening N−C_α bond cleavages triggered by radicals at the C-terminal side in **2e•** ($E_{\mathbf{TS9}}$ = 50 kJ mol^{-1}), and at the N-terminal side in **2m•** ($E_{\mathbf{TS16}}$ = 39 kJ mol^{-1}). The data indicate that proline residues in peptides can undergo ring openings that are activated by radical centers at both the N- and C-terminal sides, with TS energies that are comparable to those of other radical-induced N−C_α bond dissociations.[56] This analysis is remarkably corroborated by the recently reported statistical evaluation of ECD in a large set of tryptic peptides.[57] That work showed not only the expected effect of proline in blocking N−C_α fragmentations at the N-terminal side of proline residues, but also a greatly diminished incidence of N−C_α bond dissociations at proline C-terminal sides, in particular in peptide motifs PG, PI, and PV. Our data indicate that the facile ring opening in aminoketyl radicals flanking the proline residue can produce stable intermediates that *function as radical traps* hampering N−C_α fragmentations.[54] Our energy analysis also suggests that open-ring proline intermediates such as **2n•** can be expected to dissociate by loss of the aminoketyl H-atom that requires only 41 kJ mol^{-1}, rather than by backbone fragmentations that require higher threshold (119 kJ mol^{-1}) and TS energies. This may provide an energetically plausible explanation for the unusual behavior of proline-containing protein cation-radicals, as reported for ubiquitin.[7]

RRKM Kinetic Analysis. The calculated TS energies were used for kinetic analysis that was based on unimolecular rate constants obtained by RRKM calculations (Figure 5). These showed that the fastest unimolecular reaction of **2e•** was isomerization to **2f•** (k_1), whereas dissociations starting either from **2e•** (loss of H, k_3) or from **2f•** (C_β−$C\gamma$ bond cleavage, k_2) were notably slower. An isomerization of **2e•** to **2h•** (k_5) was faster than the loss of H, but did not lead to dissociation. An isomerization of **2e•** by amide rotation through **TS14** (k_6) became kinetically relevant at internal energies >140 kJ mol^{-1}. Note that when the system passes **TS14**, the further isomerizations through **TS15**, **TS16**, and **TS18** are spontaneous.

A conspicuous feature of the calculated rate constants was the substantial kinetic shift for reactions leading to dissociations. Figure 6 shows the calculated molar fractions of the relevant species, **2e•**, **2f•**, **2h•**, and dissociation products at 6.95 × 10^{-7} s, which was the upper bound for the experimental time scale for dissociations after the formation of **2e•** by electron transfer. The molar fractions were calculated by complete kinetic analysis of the k_1−k_6 system shown in Figure 6. The molar fraction of **2e•** showed a negligible depletion up to internal energies of E_{int} = 70 kJ mol^{-1}, after which the main depleting reaction was

(56) Tureček, F. *J. Am. Chem. Soc.* **2003**, *125*, 5954−5963.
(57) Savitski, M. M.; Kjeldsen, F.; Nielsen, M. L.; Zubarev, R. A. *Angew. Chem., Int. Ed.* **2006**, *45*, 5301−5303.

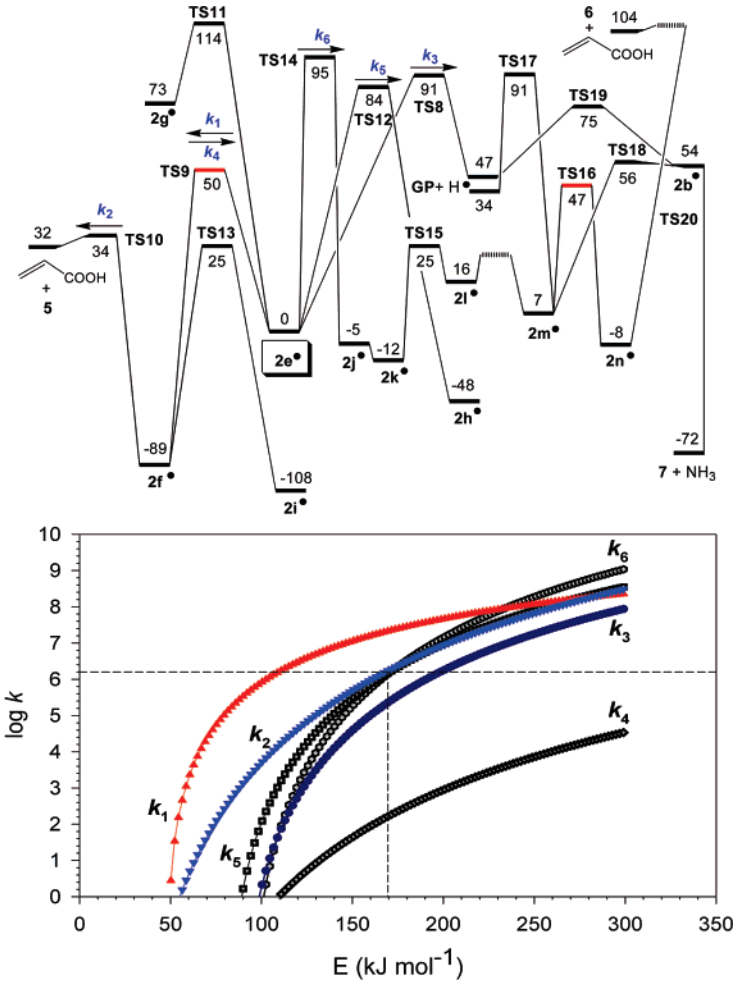

Figure 5. (Top) Potential energy surface for dissociations and isomerizations of **2e•**. The energies are from combined single-point B3LYP and PMP2/6-311++G(3df,2p) calculations and include B3LYP/6-31++G(d,p) zero-point energies. The energies (kJ mol^{-1}) are relative to **2e•** at 0 K. (Bottom) RRKM rate constants (log k, s^{-1}). The rate constants are labeled as in the top panel.

not a dissociation but ring opening to **2f•**. Furthermore, because of the kinetic stability of **2f•** and the slow isomerization of **2e•** to **2h•** and **2j•**, the *combined* molar fractions of **2e•** + **2f•** + **2h•** decreased by <5% up to internal energies of E_{int} =130 kJ mol^{-1}. The crossing point for the **2e•** and **2f•** molar fractions was found at E_{int} =103 kJ mol^{-1}. The important point of this analysis is

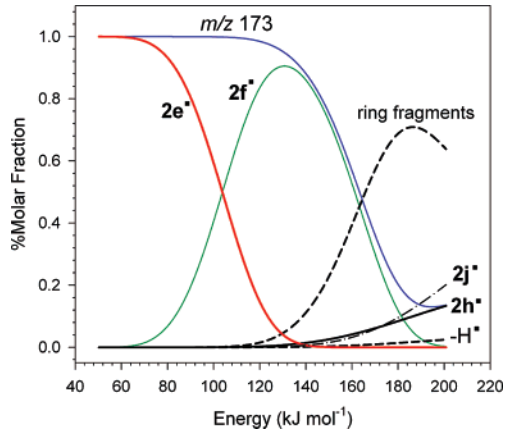

Figure 6. Branching ratios for dissociations and isomerizations of **2e•**. The *m*/*z* 173 curve represents the sum of molar fractions for **2e•**, **2f•**, **2h•**, and **2j•**. Consecutive dissociations and isomerizations of **2h•** and **2j•** were neglected in the kinetic analysis.

that radical isomers **2e•**, **2f•**, and **2h•** can give rise to stable anions by electron transfer and thus contribute to the *m*/*z* 173 peak intensity. This provides a plausible explanation for the very unusual $^{+}CR^{-}$ mass spectrum of the Gly-Pro peptide ion.

Conclusions

Radicals derived from protonated dipeptides Pro-Gly and Gly-Pro display dramatic differences in their gas-phase dissociations. While the peptide radical with the N-terminal proline dissociated spontaneously by H−atom loss, the radical with the C-terminal proline underwent H-atom rearrangement and pyrrolidine ring opening to form stable radical intermediates. Kinetic analysis of the Gly-Pro radical system indicated that ring-openings can be triggered by radical sites at both sides of the proline residue in larger peptides. These non-dissociative reactions can compete with peptide fragmentations by N−C_α bond cleavages and thus result in kinetic stabilization of the peptide radicals. Thus, isomerizations within the proline residue provide an explanation for the proline effect in electron capture and transfer dissociations.

Acknowledgment. F.T. acknowledges research support by the National Science Foundation (Grants CHE-0349595 for experiments and CHE-0342956 for computations). The Computational Chemistry Center at the UW Department of Chem-

istry receives joint support by the NSF and University of Washington.

Supporting Information Available: Complete references 9c and 14, Tables S1 and S2 with total energies and comparative test calculations for pyrrolidine cations and radicals, Tables S3−S26 with B3LYP/6-31++G(d,p) optimized geometries in Cartesian coordinate format, Scheme S1 with additional radical dissociations, and Figures S1 and S2 with auxiliary CAD and $^{+}CR^{-}$ mass spectra. This information is available free of charge via the Internet at http://www.pubs.acs.org

JA0712571